ELSEVIER

Contents lists available at ScienceDirect

Chemosphere

journal homepage: www.elsevier.com/locate/chemosphere





Enhanced malachite green photolysis at the colloidal-aqueous interface

Lukas Kaylor, Paul Skelly, Mansour Alsarrani, Mahamud Subir

Department of Chemistry, Ball State University, Muncie, IN, 47306, USA

HIGHLIGHTS

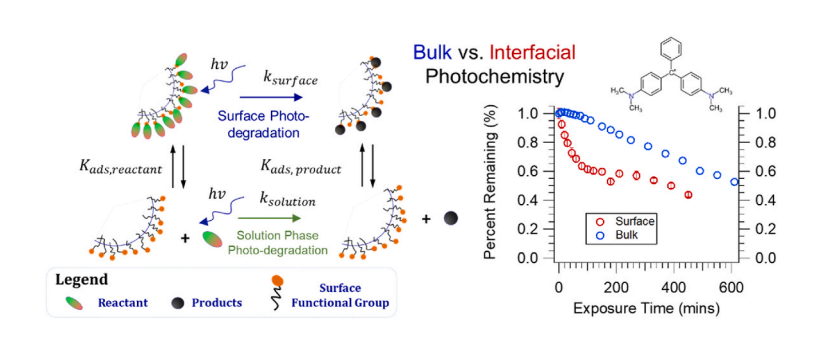
- Photodegradation of cationic malachite green (MG⁺), an organic pollutant, is enhanced at the colloidal/aqueous interface.
- MG⁺ exhibits a bathochromic shift at the surface of a non-catalytic polystyrene carboxylate (PSC) microparticle.
- N-demethylated photoinduced products of MG⁺ remain adsorbed at the PSC particle surface.
- Use of second harmonic generation to probe photokinetic and spectral properties of MG⁺ at a colloidal interface demonstrated.

ARTICLE INFO

Handling Editor: Jun Huang

Keywords:
Colloidal interface
Microplastics
Natural particulate matter
Emerging contaminants
Surface photolysis
Second harmonic generation

G R A P H I C A L A B S T R A C T



ABSTRACT

Colloids, such as natural particulate matter and microplastics, can play a significant role in the fate and transport of organic contaminants. Specifically, these small nano-to micron-sized particles provide large surface area; thus, particle-aqueous interfacial chemistry becomes significant. In this work, we present an experimental investigation of interfacial photokinetics of malachite green cation (MG⁺) adsorbed at the surface of polystyrene carboxyl (PSC) microspheres suspended in aqueous solution. Second harmonic generation (SHG), an interfacial selective laser spectroscopic tool, has been used to probe the buried interface. It is revealed that relative to the bulk, photoinduced degradation of MG⁺ is accelerated by approximately 10-fold at this noncatalytic particle surface. By measuring the SHG-based surface electronic spectra, we have also demonstrated that *N*-demethylated intermediates of MG⁺ remain at the interface until they are further decomposed. MG⁺ exhibits a bathochromic shift at the interface. Together with strong binding affinity and faster initial rate of photodegradation of MG⁺ at the interface, this work highlights that adsorption and surface photolysis are important pathways by which organic compounds can be transformed within the aquatic environment. Moreover, this research also stimulates further questions on the enrichment of reactive species at the colloidal-aqueous interface and their influence on facilitating decompositions of organic pollutants.

1. Introduction

Photolysis is an important process that plays a substantial role in dictating the fate and transport of aquatic organic contaminants and in

pollution remediation technology(Bilal et al., 2019; Olatunde et al., 2020; Wang et al., 2020). This is particularly true for synthetic industrial dyes commonly detected in environmental water(Berradi et al., 2019; Lellis et al., 2019; Yusuf, 2019). Due to their toxicity and overall

E-mail address: msubir@bsu.edu (M. Subir).

https://doi.org/10.1016/j.chemosphere.2021.131953

Received 22 June 2021; Received in revised form 27 July 2021; Accepted 18 August 2021 Available online 25 August 2021

0045-6535/© 2021 Elsevier Ltd. All rights reserved.

^{*} Corresponding author.

negative impact on the environment, photodegradation studies of various organic dyes are ubiquitous(Pérez-Estrada et al., 2008; Fischer et al., 2011; Yong et al., 2015; Ayodhya and Veerabhadram, 2018; Anwer et al., 2019). Existing photolytic studies involving organic dyes and emerging contaminants are predominantly focused on bulk aqueous phase photochemistry in the presence or absence of catalysts. However, it is recognized that dissolved organic pollutants can and do interact with various colloidal interfaces available in the aquatic environment (Murali et al., 2015; Adeyemo et al., 2017; Chianese et al., 2020; Williams et al., 2020; Bhagat et al., 2021). Examples of aquatic colloids include, but not limited to, soil and natural organic particulate matter, as well as emerging contaminants such as nanomaterials and microplastics. Adsorption of contaminants onto these colloidal surfaces and subsequent interfacial photochemistry can differ from that of the bulk solution phase photodegradation. Factors such as being subject to a distinct interfacial polarity and having reduced degree of freedom could influence the photochemical efficacy of the dye molecules upon adsorption. Accordingly, we ask the question, to what extent is the photodegradation rate altered when an organic molecule is adsorbed at a polymeric and non-catalytic colloidal-aqueous interface. Our aim has also been to gain fundamental insights into the fate of the dye and its photoinduced intermediates that may form upon photodegradation.

To this end we have performed an in situ interfacial photodegradation study of a triphenyl cationic dye, malachite green (MG⁺), adsorbed at the surface of polystyrene carboxyl (PSC) microspheres dispersed in an aquatic medium. The surface population of MG⁺ has been monitored directly upon photoexcitation without perturbing the sample. Polystyrene particles have been studied for their toxicity effect and environmental impacts and can serve as model microplastics(Wang et al., 2018; Hwang et al., 2020; Williams et al., 2020). Moreover, their uniformity in size and shape, and colloidal stability provide a unique opportunity to investigate fundamental aspects of photochemistry at the soft colloidal-aqueous interface using a light scattering spectroscopic technique used herein. Malachite green has application in aquaculture due to its fungicidal properties; however, it is potentially a health hazard, and its usage is controversial(Hashimoto et al., 2011; Gopinathan et al., 2015; Chain, 2016; Ali et al., 2020). While restricted in US and Europe, it is used in textile and other manufacturing industries in various countries. The persistence of malachite green and its metabolite in fish tissues and the aquatic environment has still been a concern in the recent years(Tan et al., 2011; Mao et al., 2018; Kwan et al., 2020). These circumstances garnered a strong motivation in investigating photochemical behavior of malachite green and resulted in a number of research study within the recent decades(Modirshahla and Behnajady, 2006; Pérez-Estrada et al., 2008; Ju et al., 2009, 2013; Fischer et al., 2011; Yong et al., 2015; Das and Dhar, 2020). The existing studies are however geared toward finding an efficient method of breaking down the organic contaminant and to understand its decolorization process in the presence or absence of catalysts or reactive oxygen species (ROS). In stark contrast with the earlier studies, MG⁺ photolysis research presented herein pertain to colloidal/aqueous interfacial photochemistry.

The main reason for the lack of interfacial photochemical studies is that it is experimentally difficult to probe the molecularly thin region between the solid particle and the aqueous phases. For instance, UV–Vis absorbance signal is not selective to the interfacial bound species. In the presence of colloids, signal from the bulk solution would dominate and thus distinguishing surface kinetics from that of the bulk becomes difficult. To circumvent this challenge, we have utilized optical second harmonic generation (SHG), a well-established spectroscopic method selective to detecting processes at buried interfaces(Eisenthal, 2006; Geiger, 2009). SHG also provides an opportunity to reveal spectra of MG⁺ and possible photoreaction intermediates at the colloidal/aqueous interface, paving the way to elucidate fate of organic contaminants in the presence of aquatic colloids. SHG has been used previously to probe adsorption of organic molecules on different kinds of colloids, including

but not limited to polymeric particles, semiconducting and metallic nanomaterials, and soft colloids(Eckenrode et al., 2005; Eisenthal, 2006; Wang et al., 2007; Gonella and Dai, 2011; You et al., 2012; Xu et al., 2015). However, until now, its utility in investigating photochemistry of organic contaminants adsorbed at the colloidal/aqueous interface has been lacking.

At this juncture it is worth emphasizing that the importance of colloids in facilitating transport of aquatic organic pollutants is wellrecognized (McCarthy, 1987; de Jonge et al., 2004; Gavrilescu, 2014). By virtue of their small size and being influenced by Brownian motion, colloids remain suspended in solutions and serve as mobile adsorbent for aquatic pollutants. Within the recent decade, adsorption of contaminants onto various organic particulate matter in soil (e.g., humus and natural organic matter) (Kennedy and Summers, 2015; Lipczynska--Kochany, 2018; Tong et al., 2019; Chianese et al., 2020; Hameed et al., 2020; Williams et al., 2020), and inorganic colloids (e.g., clays, mineral oxides, carbon based nanomaterials) (Loffredo and Senesi, 2006; Yang and Xing, 2010; Adeyemo et al., 2017; Awad et al., 2019) has been demonstrated. Interactions of dissolved organic matter with man-made and natural inorganic colloids, such as different types of oxides, has also been an active research area for which a critical review is available (Philippe and Schaumann, 2014). Adsorption studies relevant to colloidal microplastics have also emerged(Joo et al., 2021). However, many of these adsorption studies are based on separation techniques where surface bound molecules are not probed directly. In addition to the adsorption studies, research on the photolytic rates of emerging contaminants in the presence of colloidal mixtures and components of natural organic matter, e.g. humic substances, is beginning to appear (Yan et al., 2015; Cheng et al., 2018; Carena et al., 2019). These valuable research efforts serve as a motivation for the current study. However, the aim herein is to focus on the colloidal surface effect and from this perspective, the work presented herein is one of a kind. It explores surface mediated photolysis rate and intermediates formed directly, using a surface selective technique.

By means of SHG, we have measured the interfacial photolysis rate of $\rm MG^+$ under UV–Vis radiation at various surface coverage of the dye. The interfacial spectra of $\rm MG^+$, before and at an intermediate time during photolysis, have also been determined. The SHG based adsorption and photokinetic results, in comparison to the solution phase photolysis, reveal major differences between the interfacial and the bulk photochemical processes. In conjunction with the mass spectra of $\rm MG^+$ photoproducts, the SHG spectral analysis provide intriguing insights into the influence of colloids on the fate and transport of $\rm MG^+$. We begin the next section with a brief introduction on SHG and its applicability in probing colloidal-aqueous interface.

2. Materials and methods

2.1. SHG - An interfacial selective tool

SHG is a frequency doubling process. It involves simultaneous interaction between the molecule and two incident laser pulses, each at frequency ω , and a subsequent generation of light having the sum of the two incident frequencies, at 2ω . The strength of SHG intensity depends on the 2nd order susceptibility, $\chi^{(2)}$. SHG is forbidden ($\chi^{(2)}=0$) in isotropic media (e.g. bulk aqueous solution) where molecules are randomly distributed. It is allowed ($\chi^{(2)}\neq 0$) in anisotropic environment, such as the non-centrosymmetric microplastic colloidal-aqueous interface(Boyd, 2003; Shen, 2003). This means only the adsorbed dye molecules (and not the ones dissolved in solution or the amorphous polymeric microsphere themselves) can generate coherent SHG signal. Moreover, the SHG field, E_{SHG} , is directly proportional to the number density of the adsorbate, N_s (Equation (1)), where $\alpha^{(2)}_{orientation}$ is the 2nd order polarizability averaged over molecular orientation(Eisenthal, 2006).

$$E_{SHG} \propto \sqrt{I_{SHG}} \propto \chi^{(2)} \propto N_s \alpha_{orientation}^{(2)}$$
 (1)

Accordingly, relative surface population of adsorbed species can be monitored directly and *in situ* by detecting the SHG intensity, I_{SHG} . A plot of E_{SHG} vs. bulk concentration, c, of the target compound yields an adsorption isotherm. In general, incorporation of the Langmuir adsorption model in equation (1) for N_s results in Equation (2), which

provides the knowledge of the equilibrium constant, K_{ads} , representing the adsorption process. In this equation, c_0 is the molar concentration of water; i.e., 55.5 M, and E_{max} represents the plateau resulting from the surface saturation of the dye molecule.

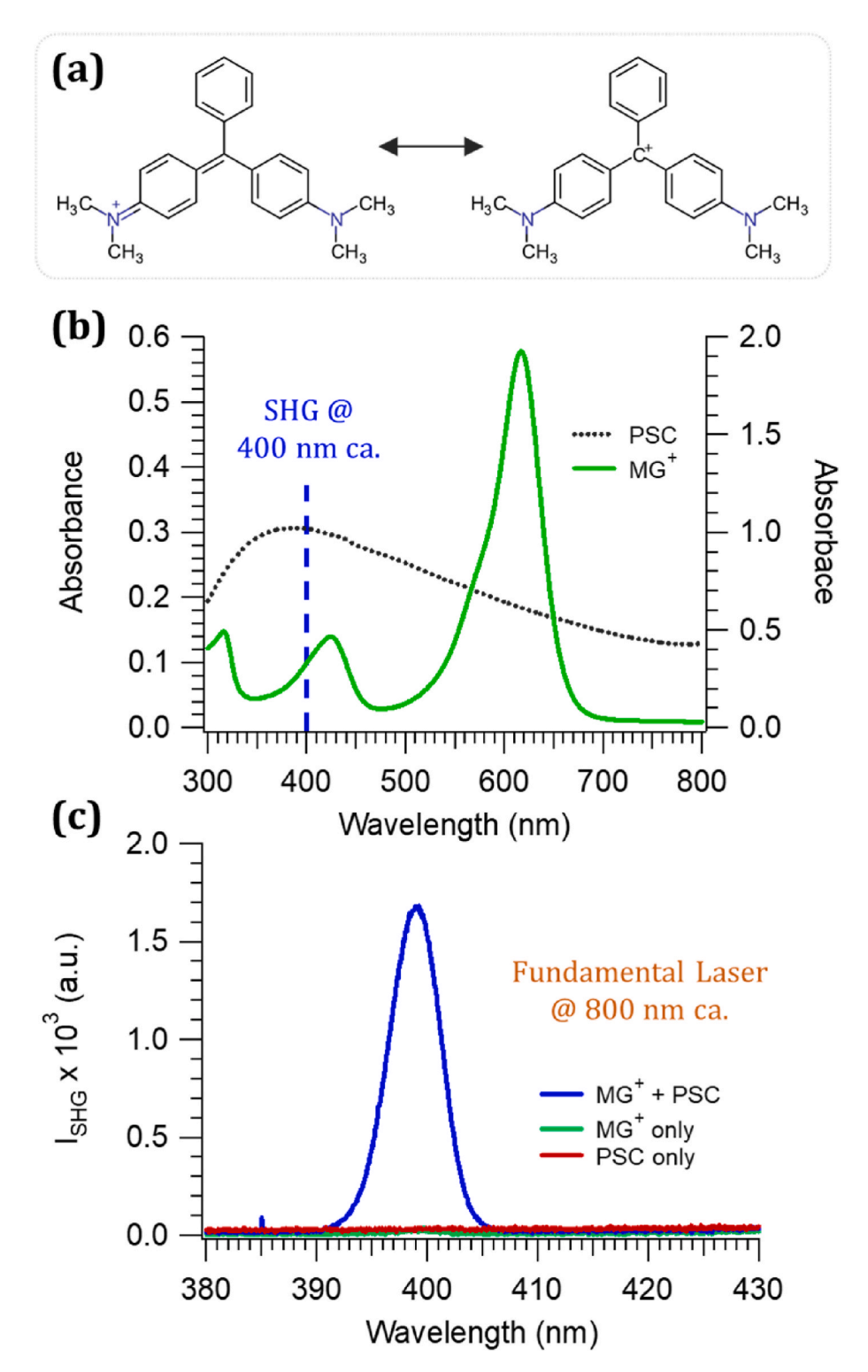


Fig. 1. (a) Resonance structures of cationic malachite green (MG^+) , (b) UV–Vis absorbance spectra of 8.5 μ M MG^+ (green trace, left axis) and PSC particle (dotted black trace, right axis) aqueous solutions, and (c) SHG signal from MG^+ adsorbed at the PSC particle-aqueous interface (blue trace) in comparison to the MG^+ (green trace) and PSC (red trace) solutions. (For interpretation of the references to color in this figure legend, the reader is referred to the Web version of this article.)

$$E_{SHG} = E_{max} \frac{K_{ads} \left(\frac{c}{c_0}\right)}{K_{ads} \left(\frac{c}{c_0}\right) + 1}$$
(2)

Another important feature of SHG is that the $\alpha^{(2)}$ term is inversely related to the transition energies as follows(Boyd, 2003; Shen, 2003):

$$\alpha^{(2)} \propto \frac{1}{\left(\omega - \omega_{gv} + i\Gamma_{gv}\right) \left(2\omega - \omega_{eg} + i\Gamma_{eg}\right)} \tag{3}$$

The denominator shows that if either ω or 2ω overlaps with the transition frequencies of the molecule, ω_{gv} and ω_{eg} , respectively, resonant enhancement of SHG intensity occurs. In practice, by tuning the wavelength of the incident laser light and thus scanning the electronic transitions of the adsorbed molecule, the surface electronic spectrum of the dye is measured. These theories provide the cornerstone for probing molecular behavior at the colloidal-aqueous and planar interfaces using SHG(Eisenthal, 2006; Geiger, 2009; Gonella and Dai, 2011). In this study, SHG has been used to determine the adsorption isotherm of MG⁺, obtain its interfacial photokinetic profiles at varying surface coverages, and measure its spectral properties before and upon photolysis.

2.2. Chemicals and materials

Polystyrene carboxyl microspheres (878 nm, diameter) and Malachite green carbinol hydrochloride (Product No. 213020, 85% dye content) were purchased from Bangs Laboratories, Inc. and Millipore Sigma, respectively. For all sample preparations, Millipore water (18.2 $M\Omega$ cm) was used. Solutions of both MG^+ and PSC were prepared with a stock solution of pH 4 prepared using HCl. A calibrated Fisher Scientific Accumet AB 150 benchtop pH meter (Fisher Scientific) was used for pH measurements. The pKa of the carboxylic functional group of the PSC particle surface is 5.4 and that of malachite green, 6.9, ensuring a predominant cationic form of malachite green(Subir et al., 2008). Fig. 1a and b shows the resonance structures of the MG⁺ and the corresponding UV-Vis spectra in solution. The light scattering from the aqueous PSC dispersion is also shown in Fig. 1b. Glassware were thoroughly cleaned using Aqua Regia (3:1 mixture of HCl and HNO3 acids) solution. For the adsorption and photokinetic studies, all MG+ and PSC samples were prepared in clean glass vials. The final mixtures of MG⁺ and PSC were prepared by 50/50 dilution of the stock MG⁺ and PSC solutions. For instance, to prepare a 10 mL mixture of 8.5 µM of MG⁺ in the presence of $1\times10^{8}~particles~mL^{-1}, 5~mL$ of 17 $\mu M~MG^{+}$ was mixed with 5 mL of $2\times$ 10⁸ particles mL⁻¹. Mixtures were vigorously vortexed. Similar approach was taken to prepare mixtures containing different concentrations of MG+ with the target particle number density. For SHG correction, the same stock solutions were used to prepare the reference samples of the dye and the PSC alone, at the desired concentration and number density, respectively. For the MG⁺ and PSC mixtures, ample time, approximately 2 h, was given for an adsorption equilibrium to reach between the dye and the particle-aqueous interface. Previous studies have shown that MG⁺ adsorption equilibrium with these particles, in the same dye concentration range, is reached in far less than 30 min(Kim, 2017). The freshly prepared mixture was used for both control (dark) and photodegraded (exposed to light) samples.

2.3. Photodegradation and second harmonic generation setup

For the photodegradation studies, a 300 W xenon-ozone free arc lamp (6258, Newport Corp.) installed with an F/1 type condenser lens was used. At the exit of the lamp, a liquid water filter (6123NS, Newport Corp.) was placed to block IR radiation and heat. A chiller (Isotemp, Fisher Scientific), set at 20 $^{\circ}C$, was used to control the temperature of the liquid filter. The output light included all possible wavelength ranging from 250 nm up to 800 nm. A previous study (Fischer et al.,

2011) in bulk solution have shown that MG⁺ photolysis photodegradation is facilitated by wavelengths shorter than 365 nm. Exposure to longer wavelengths did not find MG+ to be photolabile. The light passed through the filter and was then further collimated using a pair of lenses and an iris to a beam of ~1 cm in diameter. This beam illuminated a 1 cm quartz cuvette containing the sample under study. The cuvette was fixed within a home-built cuvette holder, which comprised of a stirring plate as the base and three flow cells in close contact around the sample cuvette. Water from the chiller was flowed through these cells using a variable flow chemical pump (Fisher Scientific) to maintain the sample under constant temperature during irradiation. This setup maintained a temperature of 22 ± 0.3 °C even under continuous exposure of at least up to 5 h. The incident power at the sample was approximately 0.5 W for all the samples studied. This corresponds to an intensity of $\sim 6.4 \times 10^3 \ W/m^2$ at the sample. The lamp was turned on at least 30 min prior to the start of photodegradation experiment. To monitor the bulk solution phase photochemistry, UV-Vis absorbance spectra were collected using Agilent Cary 8453 diode array UV-Vis

For the SHG measurements, the laser system comprised of a Ti:Sapphire ultrafast (\sim 70 fs) Tsunami oscillator optically pumped using a 532 nm CW Millennia eV. Both lasers were purchased from Spectra Physics. For the SHG-based adsorption and photokinetic studies, the fundamental wavelength was set at approximately 800 nm, which provided sufficient resonant enhancement of the SHG signal from MG⁺ adsorbed at the PSC-aqueous interface. This is due to the $S_0 \rightarrow S_2$ electronic transition in MG⁺, which peaks around 425 nm in bulk solution. Fig. 1c shows a typical SHG intensity level from a sample of MG⁺ -PSC mixture. The data also demonstrates negligible signal from the MG⁺ and PSC solutions alone, highlighting interfacial selectivity of the SHG technique.

In generating SHG, the laser beam was focused at the center of the sample contained in a quartz cuvette, which was positioned in a temperature-controlled cuvette holder (FLASH 300, Quantum Northwest). The temperature was set at $22 \, {}^{\circ}C$ and the sample was stirred. The fundamental beam from the source was attenuated and passed through various optical components such as mirrors, neutral density filters, a polarizer, a half-waveplate, a focusing lens (f = 5 cm), and a red filter. Its power immediately before the focusing lens was maintained at 500 mW and monitored to be stable throughout the duration of the experiment. The half-waveplate allowed selecting the desired polarization, vertical (V) or horizontal (H), of the incident beam, and the red filter blocked any un-wanted SHG generated from the optics. The SHG signal was passed through a blue filter (to block the fundamental beam), collimated, passed through polarizer (set at detecting vertical (V) polarized light), and focused onto the entrance of a monochromator (Acton SP2500, Princeton Instruments). SHG measurements at two different polarization input-output combinations, horizontal-vertical (HV) and vertical-vertical (VV), were conducted. The SHG intensity as a function of wavelength was collected using a CCD camera (PIXIS 400B) and processed using a WinSpec software from Princeton Instruments.

For a given data point in the photokinetic profile, SHG measurements from four distinct samples were made. They include the solutions of $\mathrm{MG^+}$ only, PSC only, the photo-exposed sample of $\mathrm{MG^+}$ -PSC mixture (sample), and the $\mathrm{MG^+}$ -PSC mixture that was kept in the dark (control). All these solutions were kept in the dark to allow adsorption to take place before starting the photodegradation experiment. Four separate quartz cuvettes were used for these samples. The control, also kept under constant stirring, provided the reference SHG signal that is not subject to degradation but captures the variation in laser power, if any, and solution condition during the entire time frame of the experiment. The other two solutions, that of $\mathrm{MG^+}$ and PSC provided intensities that were incorporated in overall correction of the SHG signal. For each sample, SHG signals from both HV and VV (input-output) polarization combinations were collected. Moreover, the UV–Vis spectra of these four

samples were also recorded after each SHG measurement using a Flame-S-UV-Vis spectrometer assembly (Ocean Optics). The absorbance values from these samples were used to correct the overall SHG intensity (See Supplemental Material for details). In brief, SHG intensities were corrected for any loss due to scattering of both fundamental and SHG light along the pathlength of the cuvette. Although negligible, the incoherent hyper-Rayleigh intensities from the MG⁺ and the PSC solutions were subtracted. To determine SHG spectra, hyper-Rayleigh intensity from acetonitrile was used a reference.

2.4. Mass spectrometry

To detect likely reaction intermediates, photodegraded samples of $\mathrm{MG^+}$ and $\mathrm{MG^+}$ -PSC were analyzed using mass spectrometry. For high resolution mass spectrometry, samples were sent to Campus Chemical Instrument Center Mass Spectrometry and Proteomics Facility at the Ohio State University. Ultrahigh resolution mass spectra and accurate mass measurements were conducted on a 15T Bruker SolariXR Fourier transform ion cyclotron resonance (FT-ICR) instrument. Ions were generated by means of electrospray ionization (ESI) in the positive ion mode. For ESI, the original (submitted) samples were dissolved in acetonitrile:water 1:1 with a 10-fold dilution. Standard ESI source conditions were used to generate the ions and previously optimized standard ion optics parameters were used for the accurate mass measurements. The mass spectrometer resolution was set to about 300,000 (at m/z 400) and the mass measurement accuracy has been estimated to be less than 2 ppm in all cases. An Agilent tune mix was used to calibrate ESI.

3. Results and discussion

3.1. Adsorption of MG+ onto PSC

A preliminary step to the interfacial photodegradation studies is the determination of MG^+ adsorption onto PSC particle. This is depicted in Fig. 2a inset. As discussed in Section 2.1, the adsorption equilibrium constant can be determined using SHG. Fig. 2b shows the SHG-based adsorption isotherms collected using two different (HV and VV) polarization combinations. The E_{SHG} data presented has been corrected for turbidity and possible re-absorption at the SHG and the fundamental wavelengths. They are presented and discussed in the Supplementary Material. We observe that the HV SHG output is greater than that of VV.

Fitting the data using Equation (2) yields K_{ads} values of $1.2~(\pm0.1)\times10^8$ and $1.3~(\pm0.1)\times10^8$ for the HV and VV combinations, respectively. The corresponding adsorption Gibbs free energy ($\Delta G_{ads} = -RTlnK_{ads}$) values are -45.7 ± 0.2 kJ/mol and -45.9 ± 0.3 kJ/mol. These values indicate a strong affinity of the MG⁺ for the neutral and negatively charged carboxyl surface moieties of the PSC microparticles. They are comparable to the values previously reported for the adsorption of MG⁺ onto different types of polymeric microspheres(Eckenrode et al., 2005).

Moreover, the good agreement in the K_{ads} values for the HV and VV measurements demonstrates that the particles do not aggregate upon $\mathrm{MG^+}$ adsorption. Adsorption equilibrium constant is pertinent to a chemical process and should not be dependent upon the polarization of the light used. In a previous study (Williams et al., 2016), it has been shown that in the presence of aggregation, the SHG signal and thereby the determination of K_{ads} can differ significantly for measurements with different polarization combinations. This was not the case here and thus, we conclude coagulation of particles upon $\mathrm{MG^+}$ adsorption is not taking place.

3.2. Surface vs. bulk MG⁺ photodegradation

The adsorption isotherm gives us an understanding of the relative surface coverage of the MG⁺ dye, which can be calculated by dividing E_{SHG} by the fitting parameter E_{max} . Based on this information, we have performed photolysis at the initial bulk MG⁺ concentration ([MG⁺]_o) of $1.7 \mu M$, $4.25 \mu M$, and $8.5 \mu M$, corresponding to the relative surface coverages of 0.76, 0.90, 0.93, respectively. Fig. 3 shows the interfacial (red markers) and the bulk solution phase (black markers) photokinetic measurements at these initial MG⁺ concentrations. Examples of UV–Vis spectra for the MG⁺, from which the bulk photokinetic profile is derived, are shown in Figure S1. The SHG-based interfacial photolysis data presented in Fig. 3 are based on HV polarization combination of the fundamental and SHG light. Similar kinetic profiles have been obtained for the VV combination. They are shown in Figure S2 of the Supplementary Material. Each of the SHG experimental data for HV and VV configurations represents an average of two independent trials. The independent trials, along with control experiments, are presented in Figures S3-S5 of the Supplementary Material. It is worth emphasizing that the HV and VV kinetic profiles are in good agreement. This indicates that there is no colloidal aggregation or a shift in the average orientation of molecules at the interface throughout the duration of photolysis.

There are two key features that are apparent when the bulk and

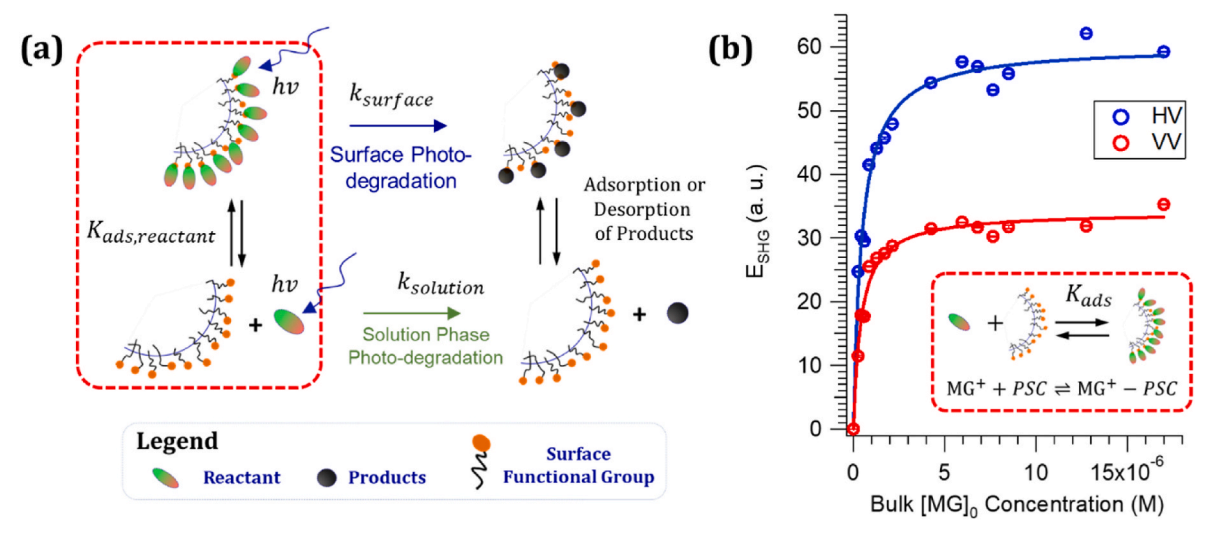


Fig. 2. (a) Schematic diagram of the processes involved in considering colloidal/aqueous interfacial photolysis and (b) SHG adsorption isotherms of MG⁺ for the PSC-aqueous interface as determined using HV and VV polarization combinations. The inset highlights the adsorption equilibrium between the reactant and the particle.

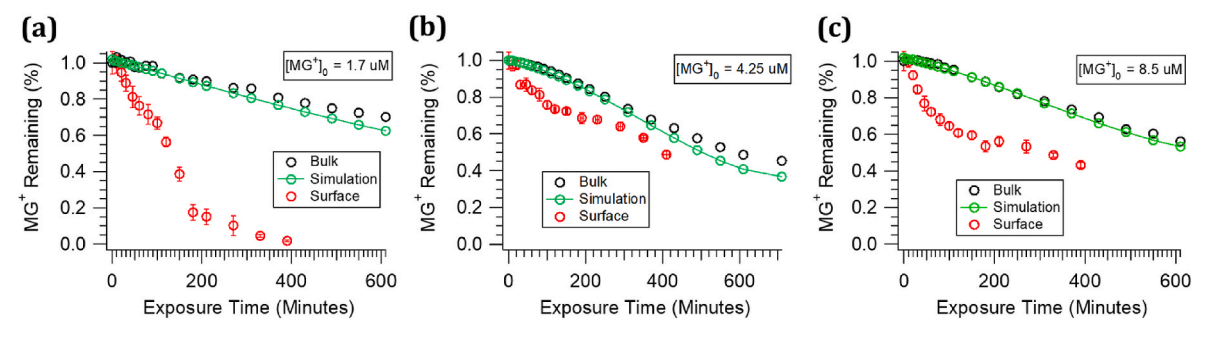


Fig. 3. Comparison of the bulk ($c/c_0vs.t$) and surface ($N/N_0vs.t$) photodegradation kinetics of MG⁺ at the initial concentration of (a) 1.7 μ M, (b) 4.25 μ M, and (c) 8.5 μ M. Also shown, simulated photokinetic profile (green lines and markers) that considers desorption of MG⁺ upon bulk degradation. The bulk solution phase and surface degradations are based on UV–Vis absorbance at 617 nm and SHG signal at HV polarization combination, respectively. (For interpretation of the references to color in this figure legend, the reader is referred to the Web version of this article.)

interfacial photo-kinetics are compared. First, it is observed that the photodegradation of interfacial bound MG^+ is faster than the corresponding bulk solution phase photodegradation. This is especially apparent at the early-time or the onset of the photoreaction and is true for all the MG^+ concentrations investigated. In all cases, including the bulk photolysis, the initial drop in the MG^+ percentage remaining is linear. Second, in the case of surface-mediated degradation, and in particular, for the higher initial MG^+ concentrations, with increasing exposure time a slow-down in the rate is apparent as photolysis progresses. More precisely, a plateau in the SHG-based kinetic profile is evident for the $[MG^+]_0$ of 4.25 and 8.5 μM . Further discussion on this unique feature is provided below.

To quantify and compare the rate of change for the surface versus bulk photodegradation, we use a linear fit to obtain a slope at the initial portion (between 0 and 80 min) for each of the photokinetic data. The initial part of the kinetic profile is generally free of interferences from the reaction intermediates and products, and in this case, the reduction in signal reflect the depletion of MG⁺. These initial rate values are given in Table 1. A clear distinction is observed with the surface rates being approximately a factor of ten larger than that of the bulk for all the concentrations studied. The fitting correlation coefficient (r) values are also tabulated, highlighting a strong correlation between the linear fit and the experimental data. As noted earlier, HV and VV kinetic profiles are similar; thus, the initial rates obtained using these polarization combinations are comparable. Within the uncertainty of the measurements, the initial photolysis rates of MG⁺ in the solution phase, as determined from the c/c_0 vs. t plot, is found to be independent of initial concentration. This is expected if the photolytic conditions are met for a pseudo first-order reaction, i.e., *ɛcl*≪1 (Logan, 1997; Levine, 2002). The extinction coefficient (ϵ) of MG $^+$ at 316 nm is in the order of 1 .4× 10⁴ M⁻¹cm⁻¹; thus, for the highest concentration studied, we have $\varepsilon cl \sim 0.1$. However, this condition does not necessarily apply when considering the photoreaction of surface bound molecules, where close to a monolayer of MG⁺ is undergoing photoreaction. Thus, a variation in

Table 1 Initial rates of surface vs. bulk MG^+ photodegradation. The fitting correlation coefficient (r) values are shown in parenthesis.

$[MG^+]_0$ ($ imes 10^{-6}~M$)	Bulk Rate $(\times 10^{-3} \text{ min}^{-1})$	Surface Rate $(\times 10^{-3} \text{ min}^{-1})$	
		HV	vv
1.7	0.43 ± 0.15 ($r = -0.708$)	3.9 ± 0.3 $(r = -0.988)$	4.8 ± 0.3 $(r = -0.990)$
4.25	0.47 ± 0.02 (r = -0.995)	2.5 ± 0.4 $(r = -0.937)$	2.9 ± 0.8 $(r = -0.860)$
8.5	$0.41 \pm 0.07 (r = -0.899)$	$4.4 \pm 0.4 (r = -0.978)$	5.2 ± 0.4 $(r = -0.987)$

the initial rates is observed with varying surface coverage.

To clarify the apparent faster photodegradation rate, we considered the possibility that the quicker extent of MG⁺ loss at the PSC-aqueous interface could be due to desorption of MG⁺ as its concentration in the solution depletes upon photolysis. Le Chatelier's principle suggests that the adsorption equilibrium (see Fig. 2b for the chemical equation) will shift to favor the reactant if the concentration of MG⁺ in the solution phase decreases. Since the MG⁺ -PSC adsorption equilibrium constant and the bulk concentration profile of MG⁺ as a function of exposure time has been determined independently (Figs. 2 and 3), it is possible to simulate the loss of interfacial MG⁺ population during the photolysis. This is shown as the green trace in Fig. 3 for each of the kinetic profiles. This simulation assumes that the surface photodegradation proceeds at the same rate as that of bulk and there is an additional loss of surface bound MG⁺ due to desorption with depletion of bulk MG⁺. As can be seen, this simulation does not predict the observed surface photokinetic of MG⁺. The reason for this miniscule desorption is the strong affinity (i. e., large K_{ads} value) of MG⁺ for the particle surface. The discrepancy highlights that the MG⁺ photolysis at the aqueous/colloid interface is fundamentally different from that of the bulk. Of particular interest is the plateau observed in the surface kinetics (Fig. 3), which we discuss next. Such plateau is not apparent in the case of bulk photolysis.

Photolysis in the presence of colloidal suspension inherently involves multiple processes. One of the processes, as highlighted in Fig. 2a, is the adsorption-desorption equilibrium of the possible intermediates and products. To elucidate the cause of the plateau, we hypothesize that an intermediate or multiple intermediate species remain at the interface and also contribute to the overall SHG. That is, SHG is mapping out not only the depletion of surface MG+ but possibly the formation of intermediates as well. Within the literature it is reported that photolytic reaction mechanism of MG⁺ predominantly proceeds via N-demethylation(Cho et al., 2003; Pérez-Estrada et al., 2008; Ju et al., 2013). The likely N-demethylated intermediates, in the order of increasing $\emph{N}\text{-demethylation},$ are monodes- \emph{MG}^+ , dides- \emph{MG}^+ , trides- \emph{MG}^+ , and tetrades- MG⁺ (see Fig. 4a). We have confirmed the formation of monodes and dides in our experimental condition. Fig. 4b shows the high-resolution mass spectra of MG⁺ after the solution is photolyzed for 150 min in the presence and absence of PSC. Both spectra show evidence of monodes- MG^+ (m/z 315.1852) formation. In the presence of PSC particles, dides- MG⁺ (301.1697) is not detected, possibly because it is adsorbed at the surface of PSC and is removed when particles are separated. Similar to MG⁺, these N-demethylated species also exhibit $S_0 \rightarrow S_2$ electronic transition in the vicinity of the SHG wavelength, 418.4 nm for monodes, and 412.3 nm and 409.9 nm for the symmetric and asymmetric dides species(Cho et al., 2003). A blueshift occurs with increasing N-demethylation. This means, if these intermediates remain adsorbed on the surface of the PSC particles, they will add to the SHG signal. Therefore, during the photolysis, a steady-state may be expected

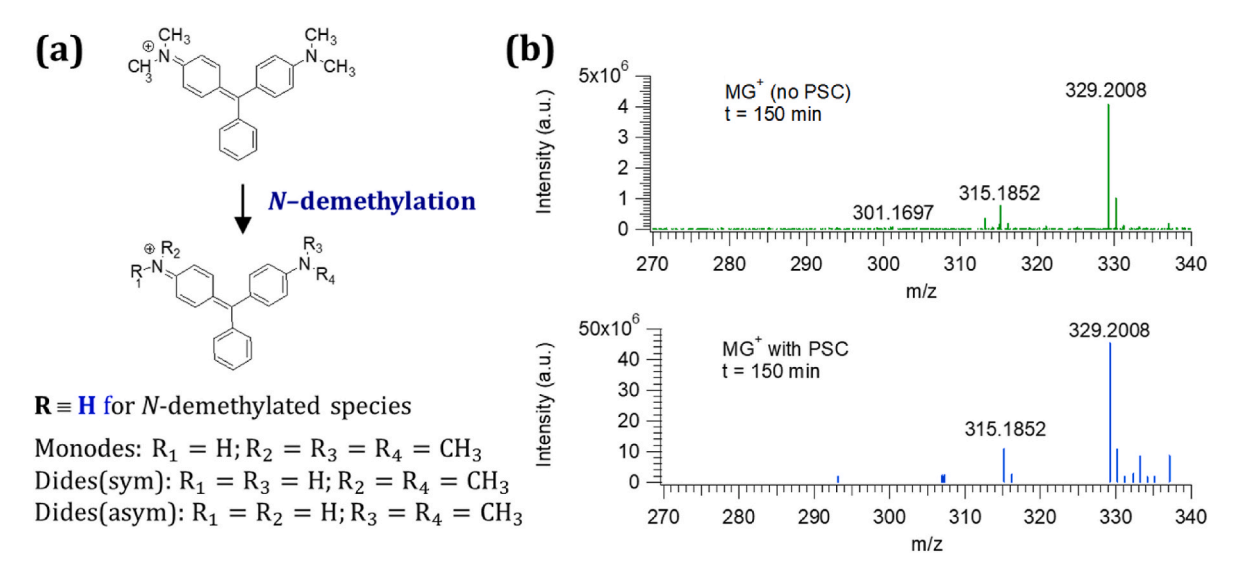


Fig. 4. (a) *N*-demethylation of MG⁺ and examples of possible *N*-demethylated intermediates. (b) High-resolution mass spectra of photolyzed MG⁺ carried out in the absence (top) and presence (bottom) of PSC particles.

between these intermediates and MG^+ . As photolysis proceeds, signal from MG^+ would decrease but formation of these intermediates would lead to a brief increase in signal until they are converted to smaller products that are no longer resonant at the SHG wavelength of 400 nm. A competition between these two sources of signal can manifest in the plateau observed in the SHG kinetic profile and then a drop-off at a longer exposure time.

3.3. Surface spectra of MG+

To verify that the intermediates are adsorbed at the PSC-aqueous interface, we have measured the surface electronic spectra of MG^+ at the particle surface after the sample has been photodegraded for 180 min and compared it to that of the un-degraded mixture. If these intermediates remain at the surface, a spectral feature at a shorter wavelength relative to the MG^+ $S_0 \rightarrow S_2$ electronic transition can be expected. The normalized surface SHG spectra, along with the solution phase UV–Vis spectra of MG^+ are presented in Fig. 5a. Indeed, we see a clear evidence of a shoulder (red markers) in the surface spectrum of the photolyzed MG^+ . Such feature is not discernible in comparing the photolyzed vs control bulk MG^+ spectra. By subtracting the normalized

SHG of the un-degraded sample from that of the degraded sample, we obtain a difference spectrum which shows a peak around 415 nm ca. This is shown in Fig. 5b. The feature and the positioning of the peak coincides very well with the transitions of the N-demethylated intermediates. Thus, by measuring the interfacial electronic spectrum of MG⁺ at the PSC/aqueous interface we have confirmed that the Ndemethylated intermediates can and do remain at the particle surface. Our hypothesis that the N-demethylated intermediates resides at the surface is thus verified. This is reasonable because these compounds would still retain the positive charge and thus, exhibit binding affinity like that of MG⁺. Based on this evidence we conclude that these intermediates are responsible for the plateau observed in the SHG-based kinetic experiments (Fig. 3), which represents a steady state between the MG⁺ and its SHG active intermediates. The fact that such plateau is not prominent for the low surface coverage case (Fig. 3a) where a sharper drop-off is seen, suggests that in this condition a sufficient buildup of the N-demethylated intermediates does not occur. Moreover, the subsequent conversion of these intermediates to smaller photoproducts is rapid relative to the bulk.

Another intriguing insight obtained from the surface spectral measurement of MG⁺ is that, compared to its bulk solution phase spectrum

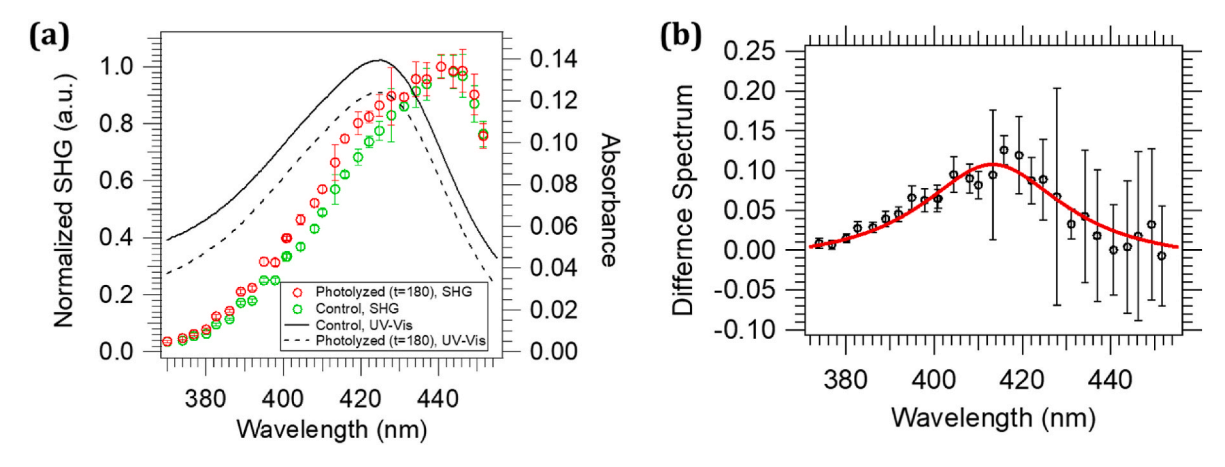


Fig. 5. (a) Surface SHG spectra (markers, left axis) of MG⁺ before (green) and after photolysis (red) overlaid with UV–Vis absorbance spectra (traces, right axis) of MG⁺ at the photolysis exposure time of t=0 (solid) and t=180 (dashed). The *x*-axis represents the UV–Vis and the SHG wavelength for the bulk and surface spectra, respectively. (b) The difference between the photolyzed and undegraded MG⁺ SHG spectra, where the solid trace is a Lorentzian fit to the experimental data. The $[\text{MG}^+]_0 = 4.25$ uM in these measurements. (For interpretation of the references to color in this figure legend, the reader is referred to the Web version of this article.)

(black trace), MG⁺ exhibits a bathochromic or a red shift (~15 nm) at the interface of the polymer particle. A similar red shift has been observed for MG⁺ adsorbed at the planar air/aqueous (Sen et al., 2010) and solid silica/water interfaces(Morgenthaler and Meech, 1993; Kikteva et al., 2000). In the case of air/aqueous interface, the shift in the wavelength has been attributed to possible formation of aggregates. A combined Brewster angle microscopy and SHG study has demonstrated aggregation of malachite green at the planar air/aqueous interface(Niu et al., 2016). However, another source for the spectral shift could be the dye's response to the changes in the polarity of the local environment. It has been suggested that the red shift at the silica surface is due to the changes in the polarity of the interfacial region; whereas, an emergence of a new broad peak at the blue side of the main transition has been associated with the adsorbate aggregation. The red-shifted spectral feature in the main electronic transition has been correlated with a more polar environment(Kikteva et al., 1999, 2000). Thus, the observed bathochromic shift suggests that the charged PSC/aqueous interface could exhibit an overall polar environment, a finding that is consistent with bathochromic shift observed for MG⁺ and other triphenylmethane dyes in the presence of micelles formed using negatively charged surfactants(Karukstis and Gulledge, 1998; Rahman et al., 2013). In our case, at the soft polymeric interface of negatively charged PSC colloids, a blue-shift or a new peak is not evident. However, the possibility of dimers that exhibit bathochromic shifts cannot be excluded. This inherently different characteristic, such as the polar nature of the interface, the restricted conformation of the strongly adsorbed dye, or the possibility of aggregates could play a role in the enhanced photodegradation rate observed.

Lastly, it is worth noting that with increasing exposure time, SHG signal once again begins to drop (Fig. 3), representing the conversion of surface bound intermediates to breakdown to smaller products, which are not resonant with the SHG wavelength. Smaller organic molecules exhibit electronic transitions at shorter wavelengths, far below the 400 nm SHG wavelength set for our experiment. Thus, they do not yield SHG signal but that does not imply that they are not at the surface. The fact that the signal decreases, and do not increase or remain steady for a longer period of time, indicates that there is no further adsorption of MG⁺ or the *N*-demethylated products from the solution to the surface of the particle. From this observation we deduce that the smaller photoproducts are also remaining at the interface such that the there is no available sites to which MG+ can adsorb. It is also possible that the surface is altered sufficiently and the proclivity of MG⁺ onto this newly coated surface is negligible. Another important implication from our findings is that an enhancement in the concentration of the photoproducts at the interfacial region is likely. These species can influence the photolytic and interfacial properties of MG⁺. Considering the mechanism of photoinduced degradation of MG⁺, if radicals are formed and are locally enriched that can further catalyze the photodegradation of MG⁺. This would in turn explain the enhanced rate observed at the surface. It has been reported that in oxygenated aqueous solution, which is the scenario in the experiments reported herein, hydroxyl radicals (HO°) are formed when malachite green is exposed to UV light(Brezová et al., 2004). The abundance of these radicals at the PSC/aqueous interface would certainly accelerate the MG+ depletion(Pérez-Estrada et al., 2008). While evidence of HO at the air/water interface has been reported (Roeselová et al., 2004; Kahan et al., 2010), further studies are needed to confirm the influence of this ROS on interfacial photochemistry in the presence of colloids.

4. Conclusion

Using SHG, an interfacial selective tool, we have discovered that cationic malachite green adsorbed at a polymeric colloidal/aqueous interface exhibits an enhanced photodegradation rate. Relative to the solution phase photolysis the initial rate at the interface is augmented by

approximately 10-fold. Moreover, interfacial SHG spectra has revealed that N-demethylated intermediates are formed and these species reside at the polystyrene carboxylate particle surface. To the best of our knowledge this is the first SHG-based electronic spectrum of MG⁺ and its intermediates upon photolysis adsorbed at the colloidal/aqueous interface. Interestingly, these intermediates also contribute to the overall SHG signal, rendering a plateau to be observed in the interfacial kinetic profile at a surface coverage close to a monolayer. While we have demonstrated that MG⁺ photodegrades at a faster rate at the colloidal interface and intermediates do buildup at the surface, we cannot pinpoint the exact source of this enhancement based on these data alone. These results however highlight the importance of photochemical interactions with noncatalytic colloids, such as microplastics, in dictating fate and transport of organic contaminants. This work prompts further investigations to elucidate the source of the enhanced rate and map out the fate of these photoproducts.

Our ongoing studies involve looking at the factors that can provide a direct explanation of the augmented rate. This includes looking at the effect of particle size, density, and reactive species on the photo-degradation rate of interfacial $\mathrm{MG^+}$ and other contaminants. A tantalizing question is whether $\mathrm{HO^{\bullet}}$ and other precursors play a role at the interface. Hydroxyl radical is an important component in the aquatic environment. While the influence of reactive species in solution phase chemistry are often reported, research on their activity at interfaces, in particular that of colloidal interfaces, are limited. To this end, exploring the affinity of hydroxyl radical species and photochemical processes under non-oxygenated environment are warranted and thus, the subjects of our future directions. We believe the findings reported herein will propel further environmental interfacial research in elucidating photochemical processes on non-catalytic colloidal interfaces.

Credit author statement

Lukas Kaylor: Investigation, Validation, Formal analysis, Visualization, Paul Skelly: Investigation, Validation, Formal analysis, Methodology, Writing – review & editing, Mansour Alsarrani: Investigation, Formal analysis, Visualization, Writing – review & editing, Mahamud Subir: Conceptualization, Methodology, Writing – original draft, Writing – review & editing, Visualization, Supervision, Project administration, Funding acquisition.

Declaration of competing interest

The authors declare that they have no known competing financial interests or personal relationships that could have appeared to influence the work reported in this paper.

Acknowledgement

This material is based upon work supported by the National Science Foundation (NSF) under Grant No. 1808468. Preliminary mass spectra were collected using support from NSF MRI Grant No. 1531851 and the ultrahigh resolution data were obtained from the 15 T Bruker SolariXR FT-ICR instrument, supported by NIH Award Number Grant S10 OD018507. We also acknowledge the American Chemical Society Petroleum Research Fund for partial support (Grant No. 53906-UNI5) in obtaining UV lamp for the photochemical study. MS is also grateful to the Ball State University ASPiRE Internal Grant Program.

Appendix A. Supplementary data

Supplementary data to this article can be found online at https://doi.org/10.1016/j.chemosphere.2021.131953.

References

- Adeyemo, A.A., Adeoye, I.O., Bello, O.S., 2017. Adsorption of dyes using different types of clay: a review. Appl. Water Sci. 7, 543–568.
- Ali, F., Bibi, S., Ali, N., Ali, Z., Said, A., Wahab, Z.U., Bilal, M., Iqbal, H.M.N., 2020. Sorptive removal of malachite green dye by activated charcoal: process optimization, kinetic, and thermodynamic evaluation. CSCEE 2, 100025.
- Anwer, H., Mahmood, A., Lee, J., Kim, K.-H., Park, J.-W., Yip, A.C.K., 2019. Photocatalysts for degradation of dyes in industrial effluents: opportunities and challenges. Nano Res. 12, 955–972.
- Awad, A.M., Shaikh, S.M.R., Jalab, R., Gulied, M.H., Nasser, M.S., Benamor, A., Adham, S., 2019. Adsorption of organic pollutants by natural and modified clays: a comprehensive review. Sep. Purif. Technol. 228, 115719.
- Ayodhya, D., Veerabhadram, G., 2018. A review on recent advances in photodegradation of dyes using doped and heterojunction based semiconductor metal sulfide nanostructures for environmental protection. Mater. Today Energy 9, 83–113.
- Berradi, M., Hsissou, R., Khudhair, M., Assouag, M., Cherkaoui, O., El Bachiri, A., El Harfi, A., 2019. Textile finishing dyes and their impact on aquatic environs. Heliyon 5 e02711–e02711.
- Bhagat, J., Nishimura, N., Shimada, Y., 2021. Toxicological interactions of microplastics/ nanoplastics and environmental contaminants: current knowledge and future perspectives. J. Hazard Mater. 405, 123913.
- Bilal, M., Adeel, M., Rasheed, T., Zhao, Y., Iqbal, H.M.N., 2019. Emerging contaminants of high concern and their enzyme-assisted biodegradation – a review. Environ. Int. 124, 336–353
- Boyd, R.W., 2003. Nonlinear Optics, second ed. Academic Press, San Diego.
- Brezová, V., Pigošová, J., Havlinova, B., Dvoranová, D., Ďurovič, M., 2004. EPR study of photochemical transformations of triarylmethane dyes. Dyes Pigments 61, 177–198.
- Carena, L., Puscasu, C.G., Comis, S., Sarakha, M., Vione, D., 2019. Environmental photodegradation of emerging contaminants: a re-examination of the importance of triplet-sensitised processes, based on the use of 4-carboxybenzophenone as proxy for the chromophoric dissolved organic matter. Chemosphere 237, 124476.
- Chain, E.Panel o.C.i.t.F., 2016. Malachite green in food. EFSA Journal 14, e04530.
 Cheng, D., Liu, X., Li, J., Feng, Y., Wang, J., Li, Z., 2018. Effects of the natural colloidal particles from one freshwater lake on the photochemistry reaction kinetics of ofloxacin and enrofloxacin. Environ. Pollut. 241, 692–700.
- Chianese, S., Fenti, A., Iovino, P., Musmarra, D., Salvestrini, S., 2020. Sorption of organic pollutants by humic acids: a review. Molecules 25, 918.
- Cho, B.P., Yang, T., Blankenship, L.R., Moody, J.D., Churchwell, M., Beland, F.A., Culp, S.J., 2003. Synthesis and characterization of N-demethylated metabolites of malachite green and leucomalachite green. Chem. Res. Toxicol. 16, 285–294.
- Das, K.C., Dhar, S.S., 2020. Remarkable catalytic degradation of malachite green by zinc supported on hydroxyapatite encapsulated magnesium ferrite (Zn/HAP/MgFe2O4) magnetic novel nanocomposite. J. Mater. Sci. 55, 4592–4606.
- de Jonge, L.W., Kjaergaard, C., Moldrup, P., 2004. Colloids and colloid-facilitated transport of contaminants in soils: an introduction. Vadose Zone J. 3, 321–325.
- Eckenrode, H.M., Jen, S.-H., Han, J., Yeh, A.-G., Dai, H.-L., 2005. Adsorption of a cationic dye molecule on polystyrene microspheres in Colloids: effect of surface charge and composition probed by second harmonic generation. J. Phys. Chem. B 109, 4646–4653.
- Eisenthal, K.B., 2006. Second harmonic spectroscopy of aqueous nano- and microparticle interfaces. Chem. Rev. 106, 1462–1477.
- Fischer, A.R., Werner, P., Goss, K.U., 2011. Photodegradation of malachite green and malachite green carbinol under irradiation with different wavelength ranges. Chemosphere 82, 210–214.
- Gavrilescu, M., 2014. Chapter 17-colloid-mediated transport and the fate of contaminants in soils. In: Fanun, M. (Ed.), The Role of Colloidal Systems in Environmental Protection. Elsevier, Amsterdam, pp. 397–451.
- Geiger, F.M., 2009. Second harmonic generation, sum frequency generation, and $\chi(3)$: dissecting environmental interfaces with a nonlinear optical Swiss army knife. Annu. Rev. Phys. Chem. 60, 61–83.
- Gonella, G., Dai, H.-L., 2011. Determination of adsorption geometry on spherical particles from nonlinear Mie theory analysis of surface second harmonic generation. Phys. Rev. B 84, 121402.
- Gopinathan, R., Kanhere, J., Banerjee, J., 2015. Effect of malachite green toxicity on non target soil organisms. Chemosphere 120, 637–644.
- Hameed, R., Lei, C., Lin, D., 2020. Adsorption of organic contaminants on biochar colloids: effects of pyrolysis temperature and particle size. Environ. Sci. Pollut. Res. 27, 18412–18422.
- Hashimoto, J.C., Paschoal, J.A.R., de Queiroz, J.F., Reyes, F.G.R., 2011. Considerations on the use of malachite green in aquaculture and analytical aspects of determining the residues in fish: a review. J. Aquat. Food Prod. Technol. 20, 273–294.
- Hwang, J., Choi, D., Han, S., Jung, S.Y., Choi, J., Hong, J., 2020. Potential toxicity of polystyrene microplastic particles. Sci. Rep. 10, 7391.
- Joo, S.H., Liang, Y., Kim, M., Byun, J., Choi, H., 2021. Microplastics with adsorbed contaminants: mechanisms and treatment. Environmental Challenges 3, 100042.
- Ju, Y., Qiao, J., Peng, X., Xu, Z., Fang, J., Yang, S., Sun, C., 2013. Photodegradation of malachite green using UV–vis light from two microwave-powered electrodeless discharge lamps (MPEDL-2): further investigation on products, dominant routes and mechanism. Chem. Eng. J. 221, 353–362.
- Ju, Y., Yang, S., Ding, Y., Sun, C., Gu, C., He, Z., Qin, C., He, H., Xu, B., 2009. Microwaveenhanced H2O2-based process for treating aqueous malachite green solutions: intermediates and degradation mechanism. J. Hazard Mater. 171, 123–132.
- Kahan, T.F., Zhao, R., Donaldson, D.J., 2010. Hydroxyl radical reactivity at the air-ice interface. Atmos. Chem. Phys. 10, 843–854.

- Karukstis, K.K., Gulledge, A.V., 1998. Analysis of the solvatochromic behavior of the disubstituted triphenylmethane dye brilliant green. Anal. Chem. 70, 4212–4217.
- Kennedy, A.M., Summers, R.S., 2015. Effect of DOM size on organic micropollutant adsorption by GAC. Environ. Sci. Technol. 49, 6617–6624.
- Kikteva, T., Star, D., Leach, G.W., 2000. Optical second harmonic generation study of malachite green orientation and order at the fused-silica/air interface. J. Phys. Chem. B 104, 2860–2867.
- Kikteva, T., Star, D., Zhao, Z., Baisley, T.L., Leach, G.W., 1999. Molecular orientation, aggregation, and order in rhodamine films at the fused silica/air interface. J. Phys. Chem. B 103, 1124–1133.
- Kim, J.H., 2017. Two-step adsorption kinetics of malachite green on anionic polystyrene microspheres in aqueous solution probed by second harmonic generation. Phys. Chem. Chem. Phys. 19, 21887–21892.
- Kwan, P.P., Banerjee, S., Shariff, M., Yusoff, F.M., 2020. Persistence of malachite green and leucomalachite green in red tilapia (Oreochromis hybrid) exposed to different treatment regimens. Food Contr. 108, 106866.
- Lellis, B., Fávaro-Polonio, C.Z., Pamphile, J.A., Polonio, J.C., 2019. Effects of textile dyes on health and the environment and bioremediation potential of living organisms. Biotechnol. Res. Innov 3, 275–290.
- Levine, I.N., 2002. Physical Chemistry. McGraw-Hill Publishing.
- Lipczynska-Kochany, E., 2018. Humic substances, their microbial interactions and effects on biological transformations of organic pollutants in water and soil: a review. Chemosphere 202, 420–437.
- Loffredo, E., Senesi, N., 2006. Fate of anthropogenic organic pollutants in soils with emphasis on adsorption/desorption processes of endocrine disruptor compounds. Pure Appl. Chem. 78, 947–961.
- Logan, S.R., 1997. Does a photochemical reaction have a reaction order? J. Chem. Educ. 74, 1303.
- Mao, Y., Yang, S., Xue, C., Zhang, M., Wang, W., Song, Z., Zhao, X., Sun, J., 2018. Rapid degradation of malachite green by CoFe₂O₄-SiC foam under microwave radiation. R. Soc. Open Sci. 5, 180085.
- McCarthy, J.F., 1987. Summary Report on Transport of Contaminants in the Subsurface: the Role of Organic and Inorganic Colloidal Particles. United States.
- Modirshahla, N., Behnajady, M.A., 2006. Photooxidative degradation of Malachite Green (MG) by UV/H2O2: influence of operational parameters and kinetic modeling. Dyes Pigments 70, 54–59.
- Morgenthaler, M.J.E., Meech, S.R., 1993. Picosecond dynamics of torsional motion in malachite green adsorbed on silica. A time-resolved surface second harmonic generation study. Chem. Phys. Lett. 202, 57–64.
- Murali, R., Murthy, C.N., Sengupta, R.A., 2015. Adsorption studies of toxic metals and dyes on soil colloids and their transport in natural porous media. Int. J. Environ. Sci. Technol. 12, 3563–3574.
- Niu, Y., Tian, K., Gan, W., Ye, S., 2016. Analyzing the stability of second harmonic intensity provides a sensitive probe of the aggregating of conjugated molecules at the interface. J. Mol. Liq. 219, 111–116.
- Olatunde, O.C., Kuvarega, A.T., Onwudiwe, D.C., 2020. Photo enhanced degradation of contaminants of emerging concern in waste water. Emerg. Contam 6, 283–302.
- Pérez-Estrada, L.A., Agüera, A., Hernando, M.D., Malato, S., Fernández-Alba, A.R., 2008. Photodegradation of malachite green under natural sunlight irradiation: kinetic and toxicity of the transformation products. Chemosphere 70, 2068–2075.
- Philippe, A., Schaumann, G.E., 2014. Interactions of dissolved organic matter with natural and engineered inorganic colloids: a review. Environ. Sci. Technol. 48, 8946–8962
- Rahman, M.M., Mollah, M.Y.A., Rahman, M.M., Susan, M.A.B.H., 2013. Electrochemical behavior of malachite green in aqueous solutions of ionic surfactants. ISRN Electrochemistry 2013, 839498.
- Roeselová, M., Vieceli, J., Dang, L.X., Garrett, B.C., Tobias, D.J., 2004. Hydroxyl radical at the Air–Water interface. J. Am. Chem. Soc. 126, 16308–16309.
- Sen, P., Yamaguchi, S., Tahara, T., 2010. Ultrafast dynamics of malachite green at the air/water interface studied by femtosecond time-resolved electronic sum frequency generation (TR-ESFG): an indicator for local viscosity. Faraday Discuss 145, 411,428
- Shen, Y.R., 2003. The Principles of Nonlinear Optics. John Wiley & Sons, Inc, Hoboken. Subir, M., Liu, J., Eisenthal, K.B., 2008. Protonation at the aqueous interface of polymer nanoparticles with second harmonic generation. J. Phys. Chem. C 112, 15809–15812.
- Tan, Z., Xing, L., Guo, M., Wang, H., Jiang, Y., Li, Z., Zhai, Y., 2011. Persistence of malachite green and leucomalachite green in perch (Lateolabrax japonicus). Chin. J. Oceanol. Limnol. 29, 647.
- Tong, Y., McNamara, P.J., Mayer, B.K., 2019. Adsorption of organic micropollutants onto biochar: a review of relevant kinetics, mechanisms and equilibrium. Environ. Sci.: Water Res. Technol 5, 821–838.
- Wang, H.-f., Troxler, T., Yeh, A.-g., Dai, H.-l., 2007. Adsorption at a carbon black microparticle surface in aqueous colloids probed by optical second-harmonic generation. J. Phys. Chem. C 111, 8708–8715.
- Wang, Y., Fan, L., Crosbie, N., Roddick, F.A., 2020. Photodegradation of emerging contaminants in a sunlit wastewater lagoon, seasonal measurements, environmental impacts and modelling. Environ. Sci.: Water Res. Technol 6, 3380–3390.
- Wang, Z., Taylor, S.E., Sharma, P., Flury, M., 2018. Poor extraction efficiencies of polystyrene nano- and microplastics from biosolids and soil. PloS One 13, e0208009.
- Williams, T., Walsh, C., Murray, K., Subir, M., 2020. Interactions of emerging contaminants with model colloidal microplastics, C60 fullerene, and natural organic matter – effect of surface functional group and adsorbate properties. Environ. Sci. Process Impacts.
- Williams, T.A., Lee, J., Diemler, C.A., Subir, M., 2016. Magnetic vs. non-magnetic colloids a comparative adsorption study to quantify the effect of dye-induced

- aggregation on the binding affinity of an organic dye. J. Colloid Interface Sci. 481,
- Xu, B., Gonella, G., DeLacy, B.G., Dai, H.-L., 2015. Adsorption of anionic thiols on silver
- nanoparticles, J. Phys. Chem. C 119, 5454–5461. Yan, C., Nie, M., Yang, Y., Zhou, J., Liu, M., Baalousha, M., Lead, J.R., 2015. Effect of colloids on the occurrence, distribution and photolysis of emerging organic contaminants in wastewaters. J. Hazard Mater. 299, 241–248.
- Yang, K., Xing, B., 2010. Adsorption of organic compounds by carbon nanomaterials in aqueous phase: polanyi theory and its application. Chem. Rev. 110, 5989-6008.
- Yong, L., Zhanqi, G., Yuefei, J., Xiaobin, H., Cheng, S., Shaogui, Y., Lianhong, W., Qingeng, W., Die, F., 2015. Photodegradation of malachite green under simulated and natural irradiation: kinetics, products, and pathways. J. Hazard Mater. 285,
- You, Y., Bloomfield, A., Liu, J., Fu, L., Herzon, S.B., Yan, E.C.Y., 2012. Real-time kinetics of surfactant molecule transfer between emulsion particles probed by in situ second harmonic generation spectroscopy. J. Am. Chem. Soc. 134, 4264–4268.
- Yusuf, M., 2019. Synthetic dyes: a threat to the environment and water ecosystem. Textiles and Clothing 11-26.